

Accepted Manuscript

Wind farm layout using Biogeography Based Optimization

Jagdish Chand Bansal, Pushpa Farswan

PII: S0960-1481(17)30074-5

DOI: [10.1016/j.renene.2017.01.064](https://doi.org/10.1016/j.renene.2017.01.064)

Reference: RENE 8503

To appear in: *Renewable Energy*

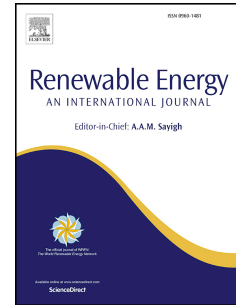
Received Date: 2 February 2016

Revised Date: 10 November 2016

Accepted Date: 30 January 2017

Please cite this article as: Bansal JC, Farswan P, Wind farm layout using Biogeography Based Optimization, *Renewable Energy* (2017), doi: [10.1016/j.renene.2017.01.064](https://doi.org/10.1016/j.renene.2017.01.064).

This is a PDF file of an unedited manuscript that has been accepted for publication. As a service to our customers we are providing this early version of the manuscript. The manuscript will undergo copyediting, typesetting, and review of the resulting proof before it is published in its final form. Please note that during the production process errors may be discovered which could affect the content, and all legal disclaimers that apply to the journal pertain.



Wind farm layout using Biogeography Based Optimization

Jagdish Chand Bansal

South Asian University, New Delhi, India

Pushpa Farswan¹

South Asian University, New Delhi, India

Abstract

Wind energy is one of the most promising option for the renewable energy. Finding optimum set of locations for wind turbines in a wind farm so that the total energy output of the farm is maximum, is usually referred as the wind farm layout optimization problem (WFLOP). This article presents the solution of WFLOP using a recent unconventional optimization algorithm, Biogeography Based Optimization (BBO). In this article, for a given wind farm not only the optimum locations of the wind turbines are obtained but also the maximum number of turbines is recommended. Experiments have been carried out for wind farms of various sizes. BBO has shown to outperform as compare to earlier methodologies of solving WFLOP.

Keywords: Wind energy, Renewable energy, Wind farm, Wind turbines, Biogeography-based optimization

1. Introduction

Wind energy is the most precious gift of nature to the world. The advance technology is trying to find out alternative of nonrenewable energy resources using wind energy. Now advance technology is developed to generate electricity from wind energy. Now a days, conventional windmills have been substituted by specially designed wind turbines for increasing the production of electricity. Wind turbine converts the wind energy into electricity.

Wind farm layout optimization (WFLO) is the pattern of wind turbines scheme subject to the constraints related to the position of the turbines, rotor radius and farm radius. In the wind farm layout optimization problem (WFLOP) model, the objective function is the maximization of expected power. The solution of this problem is to find the optimal placement of wind turbines so that the expected energy output of the whole wind farm is maximum. The complexity of WFLOP model depends on the constraints type.

The wake model depends on the thrust and the turbulence level at the turbine. The wake from one turbine will be detrimental on the wind speed and turbulence at down wind turbines. The effects of the wake spread out downwind and decay with distance according to generalized wake models. The effect of the wake is measured in the specific range. If the turbines are located within the range of four rotor diameter, they get affected by wake.

28 Significant development has been taken place in the machinery of wind energy produc-
29 tion. The percentage of wind energy production is increasing rapidly. In near future
30 also the wind energy production is expected to increase. The inherent challenge with
31 wind energy is its product cost. This challenge can be controlled by the optimal wind
32 farm layout design. Wind farm layout optimization problem is being solved from many
33 years. Researchers are continuously developing the new approaches of designing and
34 solving WFLOP. Lackner et al. [1] provided an analytical framework for offshore wind
35 farm layout optimization. Here the annual energy production of the wind farm is fully
36 dependent on the turbines position. Castro et al. [2] presented a genetic algorithm for
37 the optimal design of the wind farms. In [3], Elkinton et al. presented offshore wind
38 farm layout using several optimization algorithms. There are limited efforts done by
39 optimization community to solving WFLOP. Mosetti et al. [4] and Grady et al. [5]
40 demonstrated the placement of wind turbines using binary coded GA (genetic algo-
41 rithm) for maximizing energy production. Haung et al. [6] applied the distributed GA
42 to finding more effective optimal solution of WFLOP. Emami et al. [7] introduced a new
43 approach on optimal placement of wind turbines using GA with additional property,
44 the controlling capability of wind farm construction cost in objective function. Şişbot
45 et al. [8] used a multi-objective GA to solving WFLOP. M. Samorani [9] demonstrated
46 WFLOP consting of two conflicting problem as maximization of expected power pro-
47 duction with minimization of wake effect within several turbines. Ozturk et al. [10]
48 developed greedy heuristic methodology for wind energy conversion system positioning.
49 Bilbao et al. [11] applied simulated annealing (SA) to compute the optimal placement
50 of wind turbines in a wind farm to produce maximum power. Rivas et al. [12] also
51 applied the simulated annealing algorithm to solve wind turbine positioning problem.
52 Kusiak et al. [13] presented a generic model for wind farm layout optimization based
53 on wind distribution. In [13], evolutionary strategy is considered for optimizing layout
54 up to 6 number of turbines in the circular wind farm. Wagner et al. [14] presented
55 a better evolution strategy, named as covariance matrix adaptation based evolutionary
56 strategy (CMA-ES) for maximum power production. Yeng yin et al. [15] developed a
57 combined algorithm named as greedy randomized adaptive search procedures algorithm
58 with variable neighborhood search algorithm (GRASP-VNS) for optimal placement of
59 wind turbines. In [16] and [17], Eroğlu et al. developed ant colony optimization (ACO)
60 and particle filtering (PF) approach to solve WFLOP, respectively. These intensive uses
61 of metaheuristic algorithms to solve WFLOP inspire researchers to explore other recent
62 metaheuristics also for the same.

63 This article presents relatively a recent approach Biogeography-based optimization algo-
64 rithm (BBO) to solving WFLOP. The main objective of this article is to investigate the
65 applicability of the BBO algorithm in solving WFLOP. In this article, we try to find out
66 the optimal locations of wind turbines and maximum possible number of wind turbines
67 in the wind farms with radii 500 (m), 750 (m) and 1000 (m).

68 Rest of the article is organized as follows. The problem modeling and statement are
69 described in section 2. Section 3 details of BBO algorithm. In section 4, BBO algo-
70 rithm is applied to solve WFLOP model. In section 5, various numerical experiments,
71 comparison of results and discussions are given. The article concluded in section 6.

72 2. Problem modeling and statement

73 Some basic definitions are required to constructing the wind farm and to finding the
74 optimal placement of turbines. It is important to make some assumptions to solving the
75 WFLOP.

- 76 1. The number of turbines N is fixed before the planning of the wind farm con-
77 struction because investment in the wind farm project depends on the number of
78 turbines. For example, a 30 MW wind farm project, requires 20 number of wind
79 turbines of capacity 1.5 MW each.
- 80 2. Location of each turbine in the farm is represented in the form of two-dimensional
81 co-ordinates (x, y) and length of the location vector of each turbine is given by
82 $\sqrt{x^2 + y^2}$. Here only slight changes in surface roughness and the optimal solution
83 of WFLOP is represented by the N positions (x_i, y_i) , $i=1, \dots, N$ for N number of
84 turbines.
- 85 3. All turbines in the wind farm are considered to be uniform with respect to both
86 external quality (design, brand, model, hub height) and internal quality (power
87 curve, theoretical power, capacity).
- 88 4. For a given location, height and direction, wind speed v follows a Weibull distri-
89 bution $p_v(v, k, c) = \frac{k}{c} \left(\frac{v}{c}\right)^{k-1} e^{-\left(\frac{v}{c}\right)^k}$, where k is the shape parameter, c is the scale
90 parameter and $p_v(\cdot)$ is the probability density function. This assumption is very
91 common for many windy sites [18].
- 92 5. One of the parameter of Weibull distribution function is wind speed v which is a
93 function of wind direction θ then $v = v(\theta)$, i.e. $k = k(\theta)$, $c = c(\theta)$, $0^\circ \leq \theta \leq 360^\circ$.
94 Thus, the wind direction θ is a significant parameter of WFLOP. Fig.1 gives the
95 pictorial description of wind direction for proposed work, where $\theta = 0^\circ, 90^\circ, 180^\circ$
96 and 270° represents east, north, west and south, respectively.
- 97 6. There must be a proper space between two turbines. Proper spacing between
98 turbines reduces some dangerous loads on turbines, e.g. wind turbulence. If
99 $T_i(x_i, y_i)$ and $T_j(x_j, y_j)$ be two turbines then they should satisfy the inequality
100 $(x_i - x_j)^2 + (y_i - y_j)^2 \geq 64R^2$, where R is the given rotor radius.
- 101 7. WFLOP is a layout optimization problem. Thus the primary task of this study is
102 to consider the wind farm layout boundary. We can take elliptical, circular or any
103 other shape of the wind farm. We have selected circular shape of the wind farm
104 as a boundary for this study.
- 105 8. All the turbines must be situated within the farm. Thus any turbine T_i with
106 Cartesian coordinate (x_i, y_i) must satisfy the constraint $x_i^2 + y_i^2 \leq r^2$, where r is
107 the radius of the wind farm. In this study, wind farms of radii 500 (m), 750 (m)
108 and 1000 (m) are considered.
- 109 9. Search space of the problem is bounded by the wind farm shape and has continuous
110 coordinate variables. Therefore, to locate a wind turbine, the grid system is not
111 required.
- 112 10. Mathematical model of the problem consists of two parts: wake effect and power
113 output model. Wake effect causes lower power generation of downstream turbines.
114 The Jensen's wake model [19, 20] is used and adopted the continuous search space
115 of WFLOP. Power output model is considered from Kusiak et al. [13].

- 116 11. The objective of this study is to maximize power output in such a way that wake
 117 effect model can be minimized with two constraints obtained from assumptions 6
 118 and 8, i.e., the spacing between any two turbines is at least four rotor diameters
 119 and all turbines must be situated within the farm.

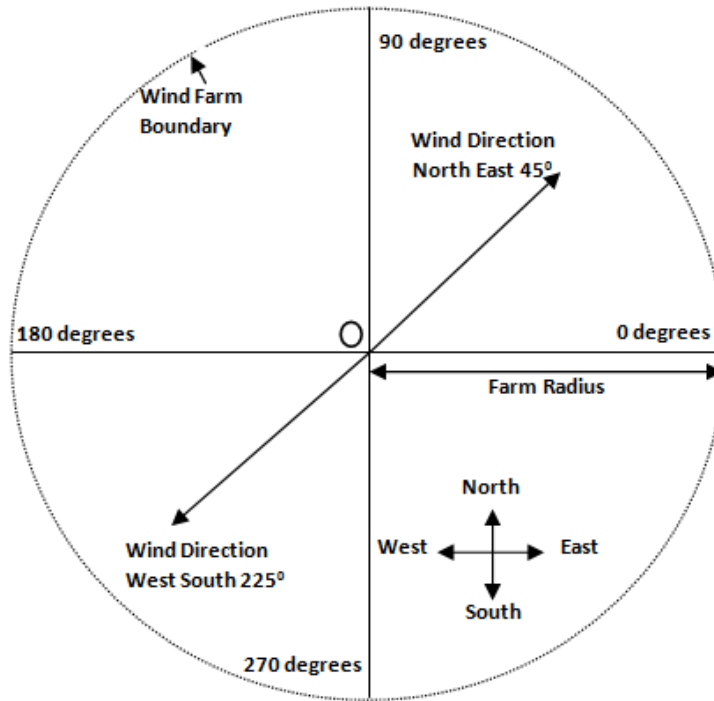


Figure 1: A typical circular wind farm with wind directions [13]

120 2.1. The wake effect model

121 Wake loss is a vital component in the wind farm layout design [21]. When a uniform
 122 wind encounters a turbine, behind the turbine, a linearly expanding wake appears [19, 1].
 123 Because of this, a part of the wind's speed will be reduced from its original speed v_{up}
 124 to v_{down} . Fig. 2 gives the pictorial description of the basic concept of the wake behind
 125 a wind turbine. Here v_{up} indicates the actual wind speed and v_{down} indicates the wind
 126 speed after wake, K indicates the wake spreading constant and d indicates the distance
 127 between two turbines.

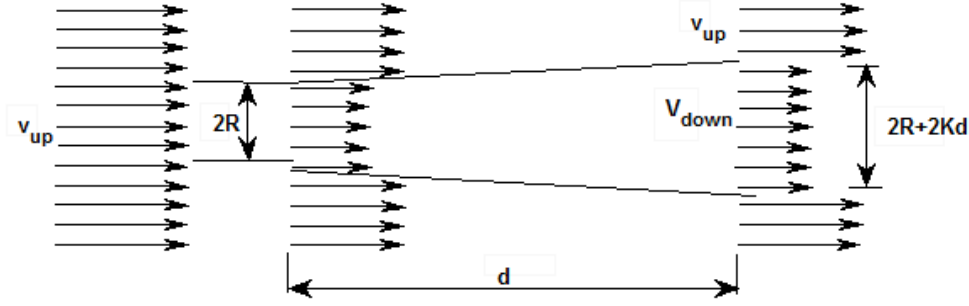


Figure 2: Wake model of wind turbine [13]

128 The velocity deficit is given by the following equation.

$$Vel_def_{ij} = 1 - \frac{v_{down}}{v_{up}} = \frac{1 - \sqrt{1 - c_T}}{(1 + Kd_{ij}/R)^2} \quad (1)$$

129 Where vel_def_{ij} indicates the velocity deficit at turbine i due to the wake of turbine j ,
 130 c_T represents the thrust coefficient of the turbine and d_{ij} indicates the distance between
 131 turbine i and turbine j , projected on wind direction θ .

132 In the case of a turbine is affected by wakes of more than one turbine. The overall
 133 velocity deficit for that turbine is calculated by the following equation.

$$Vel_def_i = \sqrt{\sum_{j=1, j \neq i}^N vel_def_{ij}^2} \quad (2)$$

134 Where vel_def_i indicates the total wind speed deficit at turbine i .

135 Given wind direction θ , all turbines' rotors are normally positioned perpendicular to
 136 the wind direction. The wake behind turbine could be seen as a part of an imaginary
 137 cone. Fig. 3, represents a half cone formed by a turbine located at (x, y) . Here A is the
 138 imaginary vertex. Parameter α ($0 \leq \alpha \leq \pi/2$) is evaluated as $\arctan(K)$.

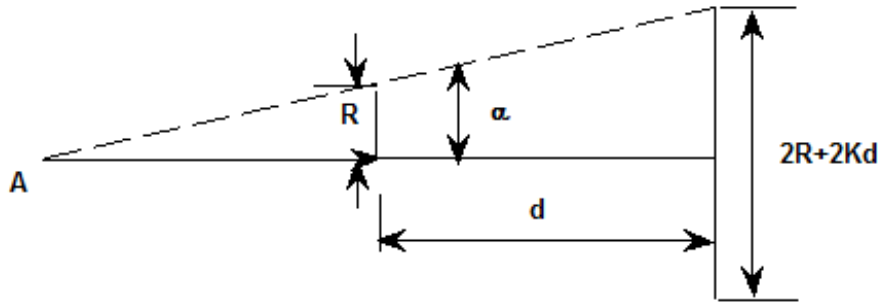


Figure 3: An imaginary half cone of a wind turbine [13]

139 **Lemma 1.** For the given wind direction θ , the angle β_{ij} , $0 \leq \beta_{ij} \leq \pi$, between
 140 vector, originating at A to turbine i and the vector, originating at A to turbine j , β_{ij} is

141 computed as

$$\beta_{ij} = \cos^{-1} \left\{ \frac{(x_i - x_j)\cos\theta + (y_i - y_j)\sin\theta + \frac{R}{K}}{\sqrt{(x_i - x_j + \frac{R}{K}\cos\theta)^2 + (y_i - y_j + \frac{R}{K}\sin\theta)^2}} \right\} \quad (3)$$

142 Where R/K indicates the distance between rotor center and A .

143 **Lemma 2.** If wind turbine i is under the wake effect of turbine j , distance between
144 turbine i and turbine j projected on the wind direction θ is,

145

$$d_{ij} = | (x_i - x_j)\cos\theta + (y_i - y_j)\sin\theta |$$

146 Equation (2) can be written as

$$Vel_def_i = \sqrt{\sum_{j=1, j \neq i, \beta_{ij} < \alpha}^N vel_def_{ij}^2} \quad (4)$$

147 Equation (4) expresses that vel_def_i is a function of wind direction θ and location of
148 turbines (x_i, y_i) .

149 Only scaling parameter c of Weibull distribution is affected by wake loss and is given by
150 equation (5) [1].

$$c_i(\theta) = c(\theta) \times (1 - vel_def_i), i = 1, \dots, N \quad (5)$$

151 Where $c_i(\theta)$ is some function of θ for a given turbine i .

152 2.2. The power model

153 The power curve model is demonstrated by following.

$$f(v) = \begin{cases} 0, & v < v_{cut-in} \\ \lambda'v + \eta, & v_{cut-in} \leq v \leq v_{rated} \\ P_{rated}, & v_{cut-out} > v > v_{rated} \end{cases} \quad (6)$$

154 Where v_{cut-in} is the cut-in wind speed. There is no power output if the wind speed is
155 less than v_{cut-in} because of low torque. The power output is static, i.e., P_{rated} if the wind
156 speed is between rated speed and cut-out speed. Power output is represented by linear
157 form between cut-in wind speed and rated wind speed. λ' expresses the slope parameter
158 and η expresses as intercept parameter.

159 The expected energy output of single turbine located at (x, y) and wind direction θ is
160 expressed as follows

$$\begin{aligned} E(P_i) &= \int_0^{360} p_\theta(\theta) E(P_i, \theta) d\theta \\ &= \int_0^{360} p_\theta d\theta \times \int_0^\infty f(v) p_v(v, k(\theta), c_i(\theta)) dv \end{aligned} \quad (7)$$

161 The objective function is to maximize the total energy production of the wind farm sub-
162 ject to assumptions (6) and (8). The optimization problem expressed by mathematical

163 model:

164

$$\begin{aligned}
 & \max \sum_{i=1}^N E(P_i) \\
 & \text{s.t.} \\
 & (x_i - x_j)^2 + (y_i - y_j)^2 \geq 64R^2, i, j = 1, 2, \dots, N, i \neq j \\
 & x_i^2 + y_i^2 \leq r^2
 \end{aligned} \tag{8}$$

165 Where $E(P_i)$ represents the power output of the i^{th} turbine. Though, $P=f(v)$ simulates
 166 a sigmoid function, it can be mathematically approximated as a linear function with
 167 tolerable error.

168 Equation (7) can be written using equation (6) and assumption (4) as follows:

$$\begin{aligned}
 E(P_i) &= \int_0^{360} p_\theta d\theta \times \int_0^\infty f(v) p_v(v, k(\theta), c_i(\theta)) dv \\
 &= \int_0^{360} p_\theta d\theta \times \int_0^\infty f(v) \frac{k(\theta)}{c_i(\theta)} \left(\frac{v}{c_i(\theta)} \right)^{k(\theta)-1} e^{-(v/c_i(\theta))^{k(\theta)}} dv \\
 &= \int_0^{360} p_\theta d\theta \times \left(\lambda \int_{v_{cut-in}}^{v_{rated}} v \frac{k(\theta)}{c_i(\theta)} \left(\frac{v}{c_i(\theta)} \right)^{k(\theta)-1} e^{-(v/c_i(\theta))^{k(\theta)}} dv \right. \\
 &+ \eta \int_{v_{cut-in}}^{v_{rated}} \frac{k(\theta)}{c_i(\theta)} \left(\frac{v}{c_i(\theta)} \right)^{k(\theta)-1} e^{-(v/c_i(\theta))^{k(\theta)}} dv \\
 &+ \left. P_{rated} \int_{v_{rated}}^\infty \frac{k(\theta)}{c_i(\theta)} \left(\frac{v}{c_i(\theta)} \right)^{k(\theta)-1} e^{-(v/c_i(\theta))^{k(\theta)}} dv \right)
 \end{aligned} \tag{9}$$

169 Wind direction is discretized into small bins so that the integration part can be approx-
 170 imated with the Riemann sum [22]. Let wind direction is discretized into $N_\theta + 1$ bins of
 171 equal width. All discretized part of wind directions between 0^0 to 360^0 are $\theta_0 = 0^0, \theta_1,$
 172 $\theta_2, \dots, \theta_{N_\theta}, \theta_{N_\theta+1} = 360^0$. Wind speed is also discretized into $N_v + 1$ bins of equal width.
 173 All discretized part of wind speed between v_{cut-in} and v_{rated} are $v_0 = v_{cut-in}, v_1, v_2, \dots,$
 174 $v_{N_v}, \theta_{N_v+1} = v_{rated}$. Finally the expected energy output of i^{th} turbine is transformed
 175 in discretized form and is given below. Detail description about this discretization of
 176 expected energy output of single turbine can be found in [13].

$$\begin{aligned}
E(P_i) = & \lambda' \sum_{j=1}^{N_v+1} \left(\frac{v_{j-1} + v_j}{2} \right) \sum_{l=1}^{N_\theta+1} \left\{ (\theta_l - \theta_{l-1}) \omega_{l-1} \right. \\
& \left. \left\{ e^{-\left(v_{j-1}/c_i \left(\frac{\theta_l + \theta_{l-1}}{2} \right) \right)^k \left(\frac{\theta_l + \theta_{l-1}}{2} \right)} - e^{-\left(v_j/c_i \left(\frac{\theta_l + \theta_{l-1}}{2} \right) \right)^k \left(\frac{\theta_l + \theta_{l-1}}{2} \right)} \right\} \right\} \\
& + P_{rated} \sum_{l=1}^{N_\theta+1} (\theta_l - \theta_{l-1}) \omega_{l-1} e^{-\left(v_{rated}/c_i \left(\frac{\theta_l + \theta_{l-1}}{2} \right) \right)^k \left(\frac{\theta_l + \theta_{l-1}}{2} \right)} \\
& + \eta \sum_{l=1}^{N_\theta+1} \left\{ (\theta_l - \theta_{l-1}) \omega_{l-1} \left\{ e^{-\left(v_{cut-in}/c_i \left(\frac{\theta_l + \theta_{l-1}}{2} \right) \right)^k \left(\frac{\theta_l + \theta_{l-1}}{2} \right)} \right. \right. \\
& \left. \left. - e^{-\left(v_{rated}/c_i \left(\frac{\theta_l + \theta_{l-1}}{2} \right) \right)^k \left(\frac{\theta_l + \theta_{l-1}}{2} \right)} \right\} \right\} \tag{10}
\end{aligned}$$

178 Where N_v expresses the number of the intervals for wind speed. N_θ expresses the num-
179 ber of the intervals for wind direction. ω_{l-1} is the blowing probability of the $(l-1)^{th}$
180 wind direction interval. The resultant optimization problem is a complex, nonlinear,
181 constrained optimization problem. Therefore, modern derivative-free optimization algo-
182 rithm becomes important to solve the model. This article uses BBO to solve the model
183 (8) with (10).

184 3. Biogeography Based Optimization

185 The popular method of studying geographical distribution of biological organisms is
186 biogeography, and whose earliest works can be traced back to the days by Alfred Wallace
187 and Charles Darwin [23]. The mathematical model of biogeography has come in the
188 picture due to Robert Mac Arther and Edward Wilson, which describes the migration of
189 species from one island to another island, the arrival of new species and the extinction of
190 some existing species [24]. Recently a new evolutionary population-based optimization
191 technique has been proposed occupying the basic nature of biogeography and is named
192 as biogeography-based optimization (BBO) [23]. However, the study of biogeography
193 contains evolution, migration and extinction but BBO is inspired by only migration
194 of species among islands. In biogeography model, the fitness of a geographical area is
195 assessed on the basis of habitat suitability index (called *HSI*). Habitats which are more
196 suitable for species to reside are said to have high *HSI*. Similarly, habitats which are less
197 suitable for species to reside are said to have low *HSI*. In this way high *HSI* habitats
198 have the relatively larger number of species. The characterization of habitability is called
199 suitability index variable (*SIVs*) for example rainfall, vegetation, temperature, etc. The
200 migration of species among different habitats is mainly controlled by two parameters,
201 immigration rate (λ) and emigration rate (μ). λ and μ are the functions of the number
202 of species in a habitat. $P_s(t)$ is the probability that there are s species in the habitat at
203 any time t .

$$P_s(t + \Delta t) = P_s(t)(1 - \lambda_s \Delta t - \mu_s \Delta t) + P_{s-1} \lambda_{s-1} \Delta t + P_{s+1} \mu_{s+1} \Delta t \tag{11}$$

204 Where λ_s is immigration rate when there are s species in the habitat. μ_s is emigration
205 rate when there are s species in the habitat.

206 At time $t+\Delta t$ one of the following condition must hold for s species in the habitat:

207

- 208 1. If there were s species in the habitat at time t . Then there will be no immigration
209 and no emigration of species within time t and $t+\Delta t$.
- 210 2. If there were $(s-1)$ species in the habitat at time t . Then one species immigrate
211 between time t and $t+\Delta t$.
- 212 3. If there were $(s+1)$ species in the habitat at time t . Then one species emigrate
213 between time t and $t+\Delta t$.

214 For ignoring the probability of more than one immigration or emigration during Δt , we
215 take Δt very small.

216 Taking $\Delta t \rightarrow 0$

$$\dot{P}_s = \begin{cases} -(\lambda_s + \mu_s)P_s + \mu_{s+1}P_{s+1}, & s = 0 \\ -(\lambda_s + \mu_s)P_s + \lambda_{s-1}P_{s-1} + \mu_{s+1}P_{s+1}, & 1 \leq s \leq s_{max} - 1 \\ -(\lambda_s + \mu_s)P_s + \lambda_{s-1}P_{s-1}, & s = s_{max} \end{cases} \quad (12)$$

217 We can obtain a matrix relation executing the dynamic equations of the probabilities of
218 the number of species in the habitat.

$$\begin{bmatrix} \dot{P}_0 \\ \dot{P}_1 \\ \vdots \\ \vdots \\ \dot{P}_{s_{max}} \end{bmatrix} = \begin{bmatrix} -(\lambda_0 + \mu_0) & \mu_1 & 0 & \cdots & 0 \\ \lambda_0 & -(\lambda_1 + \mu_1) & \mu_2 & \cdots & \vdots \\ \vdots & \ddots & \ddots & \ddots & \vdots \\ \vdots & \ddots & \lambda_{n-2} & -(\lambda_{n-1} + \mu_{n-1}) & \mu_n \\ 0 & \cdots & 0 & \lambda_{n-1} & -(\lambda_n + \mu_n) \end{bmatrix} \begin{bmatrix} P_0 \\ P_1 \\ \vdots \\ \vdots \\ P_{s_{max}} \end{bmatrix} \quad (13)$$

219 The primary concept of biogeography has been used to design a population-based opti-
220 mization procedure that can be potentially applied to optimize many engineering opti-
221 mization problems. BBO is based on the two simple biogeography concepts, migration
222 and mutation. In BBO, each habitat H represents a potential solution vector of $m \times 1$;
223 Where m is the number of *SIVs* of the habitat. We find out *HSI* of each habitat which
224 corresponds to fitness function of population-based algorithms. Habitat with highest
225 *HSI* reveals that it is the best candidate for the optimum solution among all habitats.
226 It is considered that the ecosystem constitutes N_p habitats i.e. the population size is
227 N_p . In the basic BBO algorithm, the immigration and emigration rates linearly vary
228 with number of species, as shown in Fig. 4 and they can be calculated by the following
229 formulae:

$$\lambda_j = I \left(1 - \frac{k_j}{n} \right) \quad (14)$$

230

$$\mu_j = E \left(\frac{k_j}{n} \right) \quad (15)$$

231 λ_j stands for immigration rate of j^{th} individual (island).

232 μ_j stands for emigration rate of j^{th} individual (island).

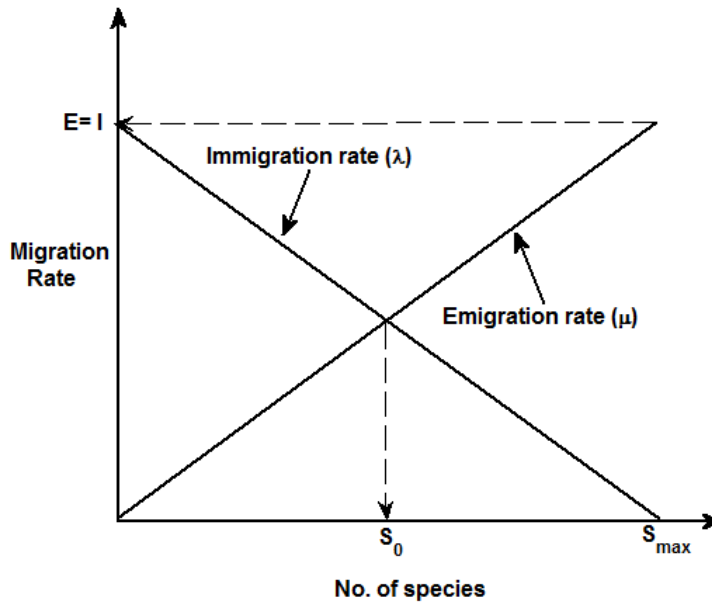


Figure 4: Relation between number of species and migration rate [23]

233 I stands for maximum possible immigration rate.

234 E stands for maximum possible emigration rate.

235 n stands for maximum possible number of species that island can support.

236 k_j stands for fitness rank of j^{th} island after sorting of fitness, so that for worst solution

237 k_j is taken as 1 and for best solution k_j is taken as n .

238 It is sufficient to assume a linear relationship between the number of species and migra-

239 tion rate for many application points of views. The relation between migration rate (λ

240 and μ) and the number of species are illustrated in Fig. 4. If there are no species in

241 the island then immigration rate is maximum, denoted by I . If there are the maximum

242 number of species (S_{max}) in the island then emigration rate is maximum, denoted by E .

243 At the state of an equilibrium number of species denoted by S_0 and in an equilibrium

244 state, immigration rate and emigration rate are equal. The islands referred as high HSI

245 islands if the number of species is more than S_0 and the islands referred as low HSI

246 islands if the number of species is less than S_0 . Algorithm 1 describes the pseudo code

247 of BBO.

248

Algorithm 1 Biogeography-based optimization algorithm

```

Initialize the population
Population size  $\leftarrow N_p$ ;
Sort the population according to the increasing order of fitness
Calculate  $\lambda$  and  $\mu$ 
Generation index  $\leftarrow GenIndex$ ;
for  $GenIndex = 1$  to  $MaxGen$  do
  Apply migration
  for  $j = 1$  to  $N_p$  do
    Select habitat  $H_j$  according to  $\lambda_j$ 
    if  $rand(0, 1) < \lambda_j$  then
      for  $e = 1$  to  $N_p$  do
        Select habitat  $H_e$  according to  $\mu_e$ 
        Replace the selected  $SIV$  of  $H_j$  by randomly selected  $SIV$  of  $H_e$ 
      end for
    end if
  end for
  Apply mutation
  for  $j = 1$  to  $N_p$  do
    Compute mutation probability  $m(S)$ 
    if  $rand(0, 1) < m(S)$  then
      Replace  $H_j(SIV)$  with randomly generated  $SIV$ 
    end if
  end for
  Sort the population according to the increasing order of fitness
  Keep the elite solution
  Stop, if termination criterion satisfied
end for

```

249 Migration and mutation are two crucial operators in BBO. “Migration” and the “Mu-
250 tation” procedures are responsible to evolve new candidate solutions. This procedure of
251 governing the habitats to the “Migration” procedure, followed by the “Mutation” pro-
252 cedure, is continued to next generation until the termination criterion is reached. This
253 criterion can be the maximum number of generations or obtaining the desired solution.
254 The basic concept of migration procedure is the probabilistically share the information
255 between habitats by utilizing the immigration rate (λ_s) and emigration rate (μ_s). The
256 migration operator is same as the crossover operator of the evolutionary algorithms and
257 is responsible for sharing the features among candidate solutions for modifying fitness.
258 In the migration procedure, immigrating habitat is selected according to the probability
259 of immigration rate and emigrating habitat is selected according to the probability of
260 emigration rate. Then probabilistically decide which of the SIV of immigrating habitat
261 is required to be modified. Once an SIV is selected, replace that SIV by emigrating
262 habitat’s SIV . The other important phenomenon is mutation. Mutation occurs by
263 sudden changes in islands due to the random event and is responsible for maintaining
264 the diversity of island in BBO process. Analysis of Fig. 4 reveals that very high HSI

265 solutions and very low *HSI* solutions have very low probability while medium *HSI* so-
 266 lutions have the relatively high probability to exist as a solution. So mutation approach
 267 gives the same chance to improve low *HSI* solutions as well as high *HSI* solutions. The
 268 mutation rate $mut(j)$ can be expressed as:

$$mut(j) = m_{max} \left(1 - \frac{P_j}{P_{max}} \right) \quad (16)$$

269 Where m_{max} is the user defined parameter and $P_{max} = \max\{P_j\}; j=1, 2, \dots, N_p$.

270 4. Biogeography-based optimization for wind farm layout optimization prob- 271 lem

272 In the literature, wind farm layout optimization problem (WFLOP) has been dealt
 273 with many nature inspired optimization algorithms, e.g. GA, PSO, PF, ACO, CMA-
 274 ES etc. Results are motivating as compare to earlier traditional approaches. BBO has
 275 already been established as one of the most promising recent continuous optimizer. To
 276 the best of authors' knowledge, BBO has yet not been applied for the solution of WFLOP.
 277 Therefore, it is significant to explore the application of BBO in solving WFLOP.

278 In a given wind farm, if N turbines are to be placed, then any arrangement of these N
 279 turbines in a two-dimensional wind farm represent a potential solution in BBO. Thus
 280 j^{th} solution x_j is represented by $x_j = (x_j^1, y_j^1, x_j^2, y_j^2, \dots, x_j^N, y_j^N)$. Clearly, the number of
 281 decision variables in the problem are $2N$. Where (x_j^t, y_j^t) for $1 \leq t \leq N$ is the position of
 282 t^{th} turbine. BBO operators are then applied to a population of such potential solutions
 283 to modify so that total energy output is maximum. The implementations of BBO to
 284 solve WFLOP is given in Algorithm 2.

Algorithm 2 BBO algorithm for WFLOP

Population size $\leftarrow N_p$;
 Generation Index $\leftarrow GenIndex$;
 Maximum number of generations $\leftarrow MaxGen$;
 Number of turbine $\leftarrow N$;
 Dimension $\leftarrow n = 2N$;
 Immigration rate $\leftarrow \lambda_{im}$
 Emigration rate $\leftarrow \mu_{em}$
 Initialize the solution $(x_j^1, y_j^1, x_j^2, y_j^2, \dots, x_j^N, y_j^N) j \leq N_p$;
 Compute $vel_def_i, c_i, E(P_i)$ for $i = 1, \dots, N$ and $\sum_{i=1}^N E(P_i)$ for each solution (habi-
 tat);
for $GenIndex = 1$ to $MaxGen$ **do**
 According to the value of λ_{im} and μ_{em} Select habitat for migration;
 Apply migration as in Algorithm 1
 Apply mutation as in Algorithm 1
 Re-compute $vel_def_i, c_i, E(P_i)$ for $i = 1, \dots, N$ and $\sum_{i=1}^N E(P_i)$ for each modified
 habitat;
 Stop, if termination criterion satisfied
end for

285 In this article, we considered two types of wind data sets (wind data set (I) given in
 286 Table 1, wind data set (II) given in Table 2). Each wind data set is distributed in 24
 287 small parts of 0 to 23 (denoted by $l - 1$). In Tables 1 and 2, wind data set is distributed
 288 in 24 intervals of wind direction (15° in each interval). In each wind direction, interval
 289 (from θ_{l-1} to θ_l), Weibull distribution shape parameter (k), Weibull distribution scale
 290 parameter (c) and wind blowing probability (ω_{l-1}) are given in Tables 1 and 2. BBO is
 291 applied with these wind data sets (Table 1, Table 2) to solve WFLOP. Considered radii
 292 of the wind farms are 500 (m), 750 (m) and 1000 (m). The number of feasible turbines
 293 varies from 2 to maximum 15 in the several wind farms. In the next section, results of
 WFLOP using BBO are reported and compared with other state of the art algorithms.

Table 1: Wind data set (I)

l-1	θ_{l-1}	θ_l	k	c	ω_{l-1}
0	0	15	2	13	0
1	15	30	2	13	0.01
2	30	45	2	13	0.01
3	45	60	2	13	0.01
4	60	75	2	13	0.01
5	75	90	2	13	0.2
6	90	105	2	13	0.6
7	105	120	2	13	0.01
8	120	135	2	13	0.01
9	135	150	2	13	0.01
10	150	165	2	13	0.01
11	165	180	2	13	0.01
12	180	195	2	13	0.01
13	195	210	2	13	0.01
14	210	225	2	13	0.01
15	225	240	2	13	0.01
16	240	255	2	13	0.01
17	255	270	2	13	0.01
18	270	285	2	13	0.01
19	285	300	2	13	0.01
20	300	315	2	13	0.01
21	315	330	2	13	0.01
22	330	345	2	13	0.01
23	345	360	2	13	0

294

295 5. Results and discussion

296 The following experimental setting is adopted to see the performance of BBO.

297 - Population size, $N_p = 50, 100$

298 - Mutation probability = 0.01

299 - Elitism size = 2

300 - Maximum immigration rate = 1

Table 2: Wind data set (II)

$l-1$	θ_{l-1}	θ_l	k	c	ω_{l-1}
0	0	15	2	7	0.0002
1	15	30	2	5	0.008
2	30	45	2	5	0.0227
3	45	60	2	5	0.0242
4	60	75	2	5	0.0225
5	75	90	2	4	0.0339
6	90	105	2	5	0.0423
7	105	120	2	6	0.029
8	120	135	2	7	0.0617
9	135	150	2	7	0.0813
10	150	165	2	8	0.0994
11	165	180	2	9.5	0.1394
12	180	195	2	10	0.1839
13	195	210	2	8.5	0.1115
14	210	225	2	8.5	0.0765
15	225	240	2	6.5	0.008
16	240	255	2	4.6	0.0051
17	255	270	2	2.6	0.0019
18	270	285	2	8	0.0012
19	285	300	2	5	0.001
20	300	315	2	6.4	0.0017
21	315	330	2	5.2	0.0031
22	330	345	2	4.5	0.0097
23	345	360	2	3.9	0.0317

301 - Maximum emigration rate = 1

302 - Maximum number of generations/iterations = 50

303 - Total number of runs/simulations = 10

304 Values of other parameters used in optimization model (8) with (10) are as below:

305 - Rotor radius, $R = 38.5$ (m)

306 - Wind cut-in speed, $v_{cut-in} = 3.5$ (m/s)

307 - Wind rated speed, $v_{rated} = 14$ (m/s)

308 - Rated power for wind speed, $P_{rated} = 1500$ (kW)

309 The parameter used in linear power curve function, $\lambda' = 140.86$, $\eta = -500$. The thrust
 310 coefficient c_T is acceded to be 0.8 and the spreading constant K is acceded to be 0.075.
 311 Wind speed is divided into $N_v = 20$ intervals of 0.5 (m) each, where the initial point
 312 is v_{cut-in} and final point is v_{rated} . Similarly, the wind direction is divided into $N_\theta = 23$
 313 intervals of 15° each.

314 For the wind data set (I), given in Table 1 the Weibull parameters ($k=2$ and $c=13$)
 315 are fixed in each interval of wind direction. But the wind blowing probability varies in
 316 several wind directions. Wind blowing probability in initial wind direction (from 0° to
 317 15°) and in last wind direction (from 345° to 360°) is 0 ($\omega_0 = 0$ and $\omega_{23} = 0$). The wind
 318 blowing probability is the highest in the wind direction interval from 75° to 105° . In the

319 wind direction interval from 75° to 90° , the wind blowing probability is 0.2 ($\omega_5 = 0.2$)
 320 and in the wind direction interval from 90° to 105° , the wind blowing probability is 0.6
 321 ($\omega_6=0.6$). The wind blowing probability in other wind direction is 0.01 ($\omega_l=0.01$, $l \neq 0$,
 322 5, 6, 23).

323 For the wind data set (II) given in Table 2, shape parameter is fixed ($k = 2$) but Weibull
 324 distribution scale parameter (c) is not fixed in each interval of the wind direction. The
 325 lowest value of scale parameter (c) is 3, in the wind direction interval (from 255° to 70°)
 326 and the highest value of c is 10 in two wind direction intervals (from 165° to 180° and
 327 180° to 195°).

328 Since the power production is directly proportional to the number of wind turbines.
 329 Therefore, for a given wind farms sizes, we wish to find out maximum limit of the fea-
 330 sible wind turbines and their placements with minimum wake loss or maximum power
 331 output. The results using BBO for considered farm radii (500 (m), 750 (m) and 1000
 332 (m)) are discussed below.

333

334 **Wind farm radius 500 (m):** Tables 3 and 4, illustrate the expected power with
 335 wake loss in the farm radius 500 (m) for the wind data set (I) and the wind data set
 336 (II), respectively. In Tables 3 and 4, columns 1 and 2 report the number of turbines
 337 and the ideal expected power corresponding to the number of turbines. Results of wind
 338 data sets (I) and (II) from earlier studies are reported in column 3 - 7. Evolutionary
 339 algorithm (EA) results (column 3), Ant colony optimization (ACO) (columns 4 and 5)
 340 and Particle filtering (PF) approach results (columns 6 and 7) are reproduced from [13],
 341 [16] and [17], respectively. In Tables 3 and 4, columns 8 and 9 report the best-expected
 342 power with wake loss for 50 population size ($50 N_p$) and 100 population size ($100 N_p$)
 343 corresponding to the number of turbines using BBO algorithm. Finally in Tables 3
 344 and 4, columns 10 and 11 report the average of expected power with wake loss in 10
 345 runs for 50 population size ($50 N_p$) and 100 population size ($100 N_p$) corresponding to
 346 the number of turbines using BBO algorithm. Previously, many approaches have been
 347 applied to calculate maximum expected power production of wind turbines. In [13],
 348 Andrew and Kusiak solved this problem by the evolutionary algorithm (EA) and able
 349 to find the optimal placement of 6 turbines on farm radius 500 (m). Authors were in
 350 the view that there is no more optimal space for more than 6 turbines in the same farm
 351 area for both wind data sets (wind data set (I) and wind data set (II)). Then in [16],
 352 Eroğlu and Seçkiner developed the efficient solution by ant colony optimization (ACO)
 353 and succeeded to find the optimal location of maximum 8 number of turbines on the
 354 same wind farm. In ACO, the ideal expected power is compared with ACO (best) and
 355 ACO (average of 10-run). From the Tables 3 and 4, it is clear that up to 3 turbines,
 356 best-expected power output is equal to the ideal expected power output. Again in [17],
 357 Eroğlu and Seçkiner improved the optimal position of wind turbines using particle fil-
 358 tering (PF) approach. From the comparison data given in Tables 3 and 4, PF approach
 359 is better than EA and ACO algorithm. But still the best-expected power is not equal to
 360 the ideal expected power (optimum) for more than 3 turbines. These two solutions mo-
 361 tivate authors to explore the performance of BBO to WFLOP. It is expected that BBO
 362 could provide the optimal placement of more turbines on the same farm. Tables 3 and 4
 363 show the comparison of expected power and wake loss developed by EA, ACO, PF and
 364 BBO algorithm. Table 3 shows that up to 7 turbines, the best-expected power is equal

365 to the ideal expected power but 8 turbines can be placed with the negligible amount
366 of wake loss. But Table 4 shows that up to 6 number of turbines, the best-expected
367 power is equal to the ideal expected power but 7 and 8 turbines can be placed with the
368 negligible amount of wake loss.

369 In this way, we can not place more than 8 turbines on the wind farm of radius 500 (m).
370 Therefore expected power generation capacity of wind farm of radius 500 (m) using BBO
371 algorithm is better than EA, ACO and PF approach.

372 Figures 5 and 6, illustrate the optimum location of wind turbines from 2 to 8 turbines for
373 the wind data set (I) and the wind data set (II), respectively. Here in figures 5(a)-5(g)
374 and 6(a)- 6(g), turbines' best position is seen for the best-expected power (column 8)
375 given in Tables 3 and 4, respectively.

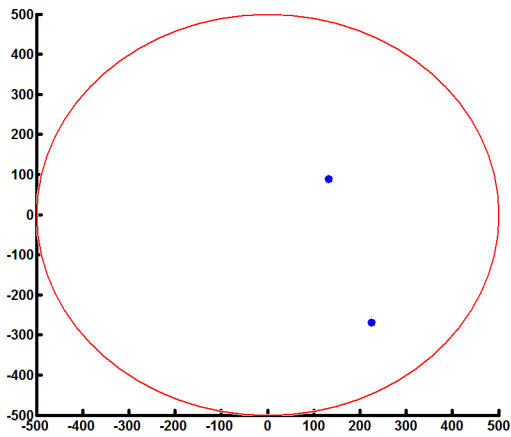
376 The change in wake loss with respect to iterations can be observed using fitness curve
377 in figures 7 and 8. Fitness curve for wind data sets (I) and (II) with population size 50
378 are given in figures 7(a) and 7(b), respectively. Similarly the fitness curve with popu-
379 lation size 100 are given in figures 8(a) and 8(b), respectively. Only for feasible fitness
380 values, fitness curves are shown. It can be easily observed that within 50 iterations, the
381 fitness curve becomes parallel to the horizontal axis, i.e. the chances of further improve-
382 ment are negligible. Thus 50 iterations seems to be sufficient for experiments. For 2, 3
383 and 4 turbines cases, the optimum solution is reached in early iterations and therefore
384 corresponding fitness curves are not shown here.

Table 3: Expected power and wake loss (*in kW*) in the wind farm of radius 500 (*m*) for the wind data set (I)

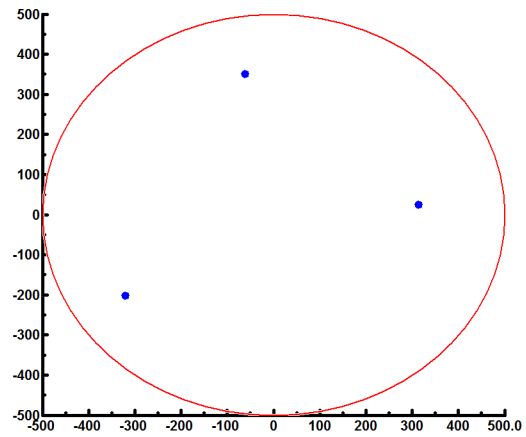
Number of turbines	Ideal	EA	ACO (best)	ACO (average of 10-run)	PF (best)	PF (average of 10-run)	BBO (best)		BBO (average of 10-run)	
							/Wake Loss		/Wake Loss	
							50 N_p	100 N_p	50 N_p	100 N_p
2	28091.47	28083.42 /8.05	28091.47 /0	28091.47 /0	28091.47 /0	28091.47 /0	28091.47 /0	28091.47 /0	28091.47 /0	28091.5 /0
3	42137.21	42101.06 /36.15	42137.21 /0	42130.87 /6.34	42137.21 /0	42128.32 /8.89	42137.21 /0	42137.21 /0	42137.21 /0	42137.2 /0
4	56182.95	56057.77 /125.18	56150.13 /32.82	56128 /54.95	56152.58 /30.37	56135.28 /47.67	56182.95 /0	56182.95 /0	56167.85 /15.1	56171.1 /11.89
5	70228.69	69922.97 /305.72	70113.48 /115.20	70086.29 /142.40	70122.64 /106.05	70085.66 /143.03	70228.69 /0	70228.69 /0	70196.42 /32.27	70207.2 /21.53
6	84274.42	83758.79 /515.63	84042.34 /231.09	84006.37 /268.05	84047.05 /227.37	84007.84 /266.58	84274.42 /0	84274.42 /0	84236.19 /38.23	84167.4 /106.98
7	98320.16	—	97905.99 /414.17	97822.66 /497.50	97918.69 /401.47	97869.73 /450.43	98320.16 /0	98320.16 /0	98265.71 /54.45	98280.5 /239.71
8	112365.9	—	111589.7 /776.20	111414.82 /951.08	111694.24 /671.66	111498.83 /867.07	112318.78 /47.12	112322.9 /43.01	112168.34 /197.56	111894 /471.99
9	126411.64	—	—	—	—	—	Infeasible	Infeasible	Infeasible	Infeasible

Table 4: Expected power and wake loss (*in kW*) in the wind farm of radius 500 (*m*) for the wind data set (II)

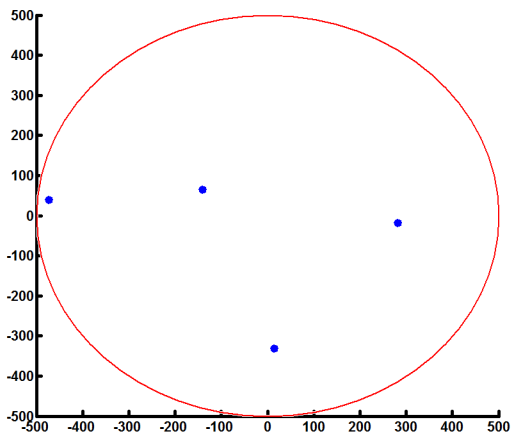
Number of turbines	Ideal	EA /Wake Loss	ACO (best) /Wake Loss	ACO (average of 10-run) /Wake Loss	PF (best) /Wake Loss	PF (average of 10-run) /Wake Loss	BBO (best) /Wake Loss		BBO (average of 10-run) /Wake Loss	
							50 N_p	100 N_p	50 N_p	100 N_p
							2	14631.37	14631.21 /0.16	14631.37 /0
3	21947.06	21925.16 /21.90	21947.06 /0	21928.07 /18.99	21947.06 /0	21915.78 /31.28	21947.06 /0	21947.06 /0	21947.06 /0	21947.06 /0
4	29262.75	29,113.71 /149.04	29,204.65 /58.10	29,174.20 /88.55	29217.83 /44.92	29182.38 /80.37	29262.75 /0	29262.75 /0	29232.54 /30.21	29232.74 /30.01
5	36578.44	36,316.23 /262.21	36,389.27 /189.16	36,256.10 /322.34	36421.55 /156.89	36284.07 /294.37	36578.44 /0	36578.44 /0	36507.35 /71.09	36508.67 /69.77
6	43894.12	43,195.84 /698.28	43,202.50 /691.62	43,125.19 /768.93	43326.88 /567.24	43181.70 /712.42	43894.12 /0	43894.12 /0	43795.59 /98.53	43697.25 /196.87
7	51209.81	—	49,943.97 /1265.84	49,763.76 /1446.06	50011.33 /1198.48	49819.71 /1390.10	51208.05 /1.76	51209.81 /0	50993.02 /216.79	50914.72 /295.09
8	58525.50	—	56,453.73 /2071.77	56,316.15 /2209.35	56664.57 /1860.93	56498.03 /2027.47	58401.71 /123.79	58468.88 /56.62	58128.58 /396.92	58020.39 /505.11
9	65841.19	—	—	—	—	—	Infeasible	Infeasible	Infeasible	Infeasible



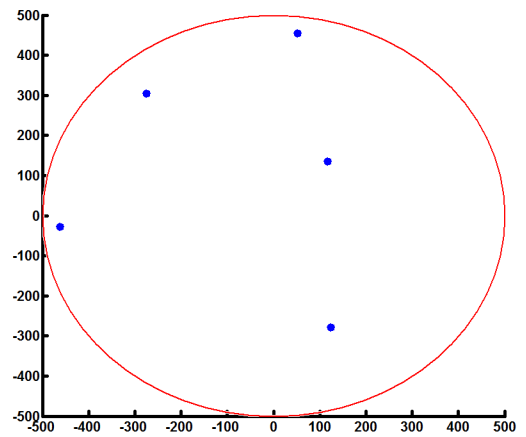
(a) 2 turbine



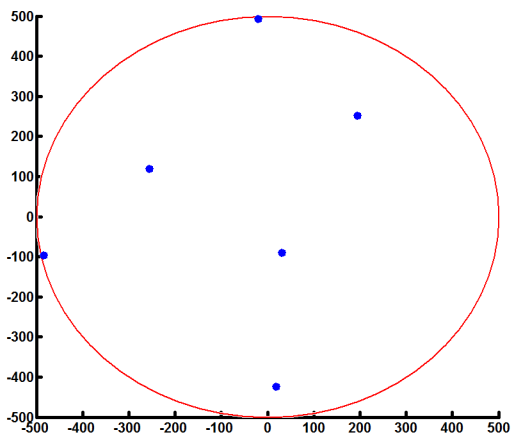
(b) 3 turbine



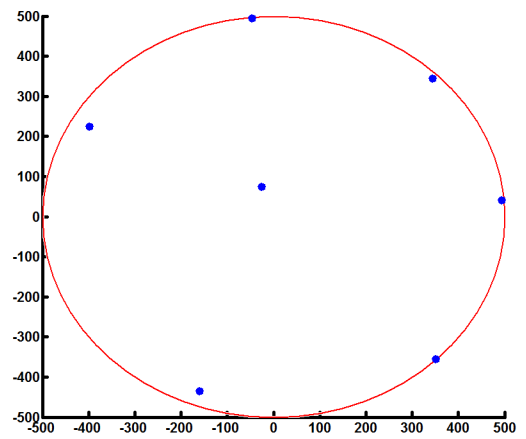
(c) 4 turbine



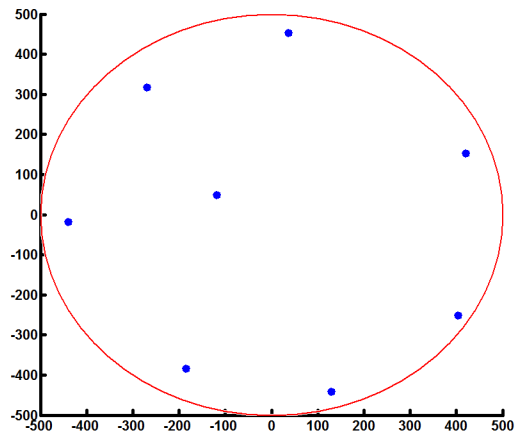
(d) 5 turbine



(e) 6 turbine

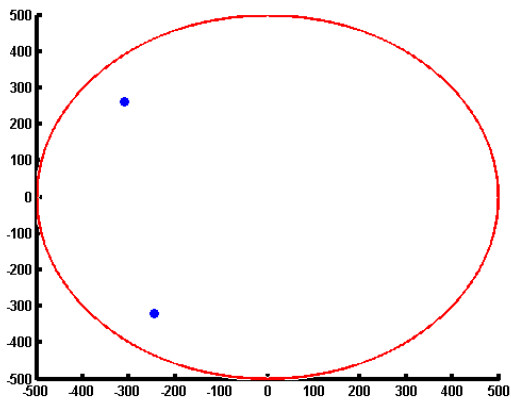


(f) 7 turbine

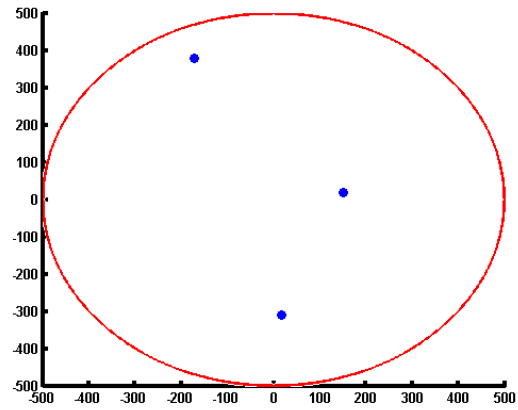


(g) 8 turbine

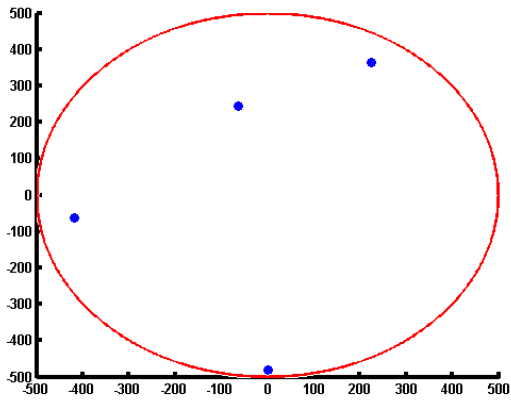
Figure 5: Turbines' location in the wind farm of radius 500 (m) for the wind data set (I)



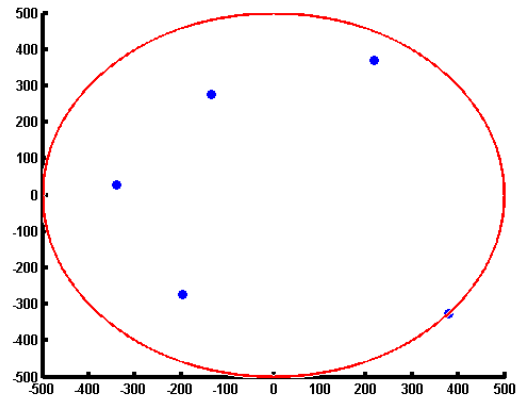
(a) 2 turbine



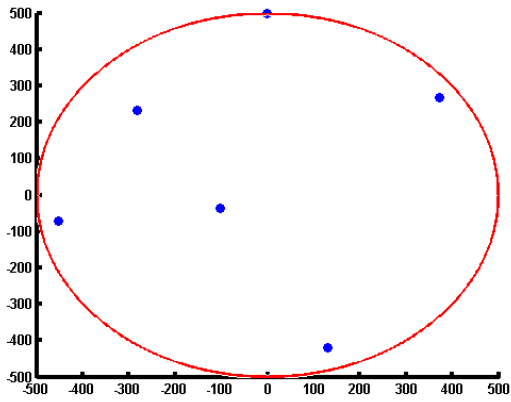
(b) 3 turbine



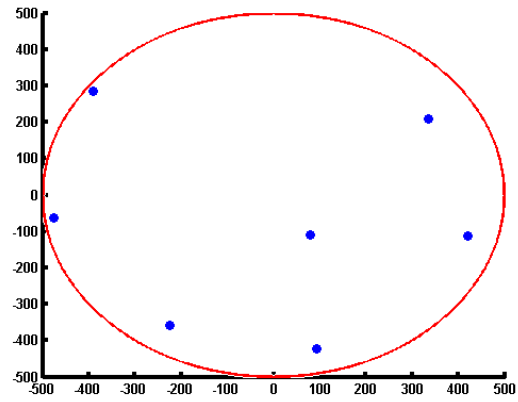
(c) 4 turbine



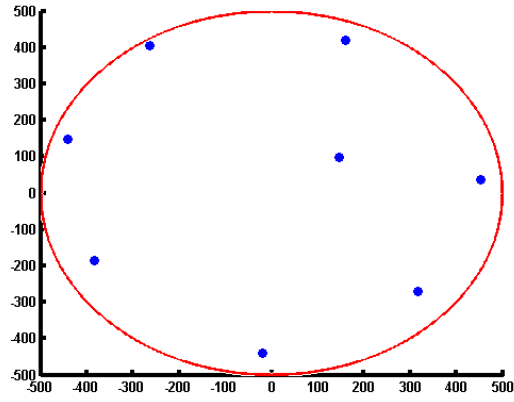
(d) 5 turbine



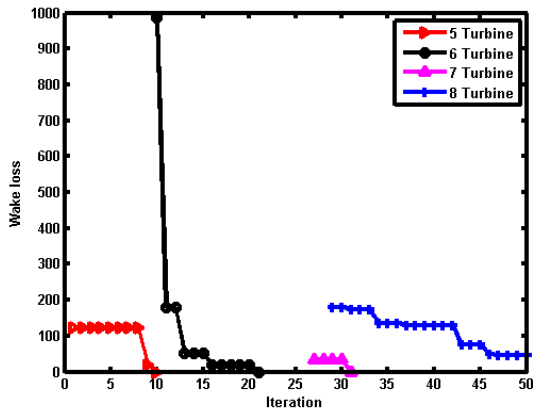
(e) 6 turbine



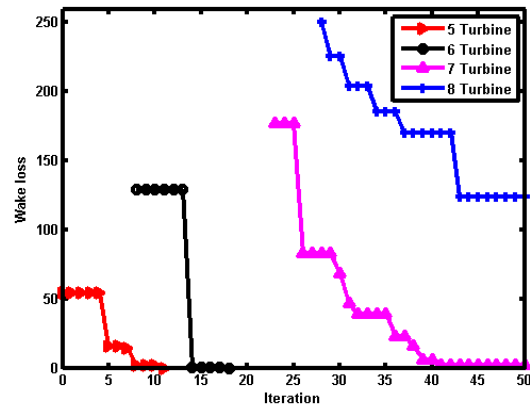
(f) 7 turbine



(g) 8 turbine

Figure 6: Turbines' location in the wind farm of radius 500 (m) for the wind data set (II)

(a) Wake loss vs iteration for the wind data set (I)



(b) Wake loss vs iteration for the wind data set (II)

Figure 7: Fitness curve for the wind farm of radius 500 (m) with $N_p = 50$

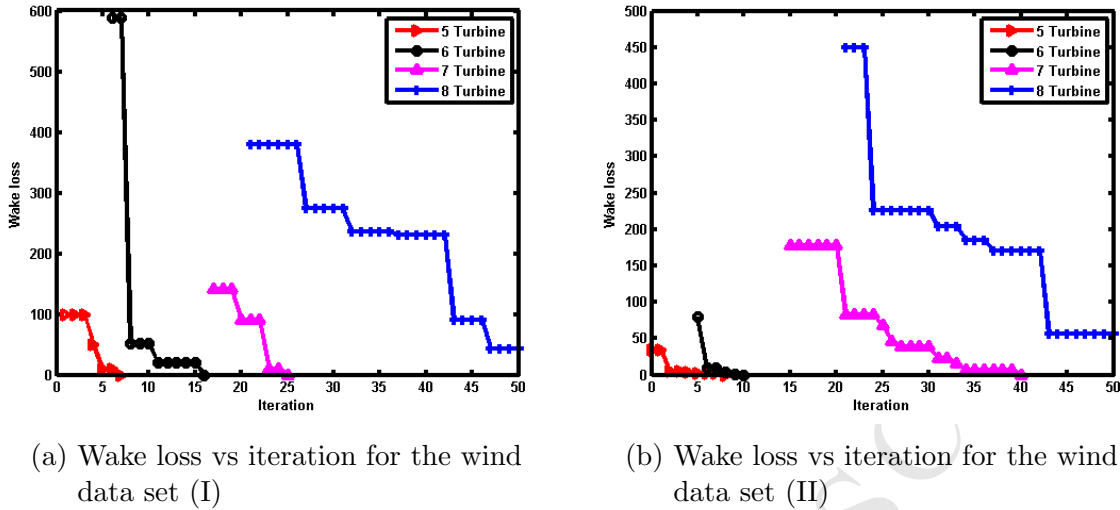


Figure 8: Fitness curve for the wind farm of radius 500 (m) with $N_p = 100$

385 **Wind farm radius 750 (m):** We succeeded to find the optimal placement of only
 386 up to 7 turbines for the wind data set (I) and up to 6 turbines for the wind data set
 387 (II) in the wind farm of radius 500 (m) without any wake loss. So we require more
 388 space to establish the wind turbines without any wake loss. In this way searching the
 389 possibility of the optimal placement of more turbines, farm radius is increased by 250
 390 (m). Now further searching for the optimal placement of more number of turbines
 391 and also find the maximum possible limit of the feasible wind turbines on the wind farm
 392 of radius 750 (m). In Tables 5 and 6, columns 1 and 2 report the number of turbines
 393 and the ideal expected power corresponding to the number of turbines. In Tables 5 and
 394 6, columns 3 and 4 report the best-expected power with wake loss for 50 population
 395 size ($50 N_p$) and 100 population size ($100 N_p$) corresponding to the number of turbines
 396 using BBO algorithm. Finally in Tables 5 and 6, columns 5 and 6 report the average
 397 of expected power with wake loss in 10 runs for 50 population size ($50 N_p$) and 100
 398 population size ($100 N_p$) corresponding to the number of turbines using BBO algorithm.
 399 Table 5 illustrate the best-expected power, expected power of average of 10-run and
 400 wake loss up to 12 number of turbines for the wind data set (I) and data is compared
 401 with only the ideal expected power (optimum) because no data available in the literature
 402 for this wind farm size. In the wind farm of radius 500 (m), wake loss is measured if 8
 403 number of turbines establish but no wake loss is found in the wind farm of radius 750
 404 (m) up to 9 number of turbines for the wind data set (I). As well as Table 6 illustrates
 405 the best-expected power, expected power of average of 10-run and wake loss up to 12
 406 turbines for the wind data set (II) and data is compared with only the ideal expected
 407 power (optimum) because no data available in the literature for this wind farm size. In
 408 the wind farm of radius 500 (m), wake loss is measured if 7 number of turbines establish
 409 but no wake loss is found in the wind farm of radius 750 (m) up to 8 number of turbines
 410 for the wind data set (II). In the wind farm of radius 750 (m) only up to 12 number
 411 of turbines can be established. Tables 5 and 6 clear the maximum limit of the feasible
 412 number of turbines for specific wind farm radius 750 (m) can not be exceeded by 12
 413 number of turbines.

414 Fig. 9, illustrates the optimum location of wind turbines from 8 to 12 turbines. Here in
 415 figures 9(a)-9(e), turbines' best position is seen for the best-expected power (column 3)
 416 given in Table 5. Again Fig. 10, illustrates the optimum location of wind turbines from
 417 7 to 12 number of turbines. Here in figures 10(a)-10(f), turbines' best position is seen
 418 for the best-expected power (column 3) given in Table 6.
 Similar to 500 (m) farm case, fitness curves are shown in figures 11 and 12.

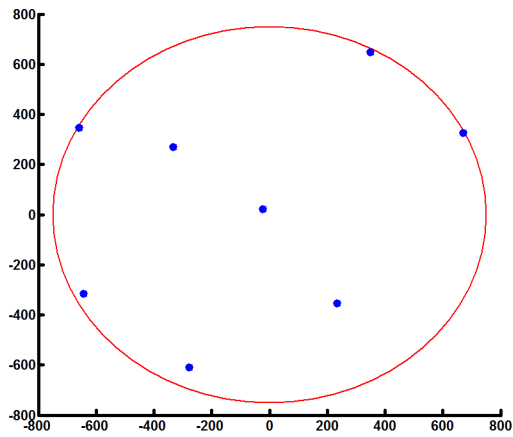
Table 5: Expected power and wake loss (*in kW*) in the wind farm of radius 750 (m) for the wind data set (I)

Number of turbines	Ideal	BBO (best)		BBO (average of 10-run)	
		/Wake Loss		/Wake Loss	
		50 N_p	100 N_p	50 N_p	100 N_p
2	28091.47	28091.47	28091.47	28091.47	28091.47
3	42137.21	/0	/0	/0	/0
		42137.21	42137.21	42137.21	42137.21
4	56182.95	/0	/0	/0	/0
		56182.95	56182.95	56182.95	56182.95
5	70228.69	/0	/0	/0	/0
		70228.69	70228.69	70228.69	70228.69
6	84274.42	/0	/0	84261.58	84245.1
		84274.42	84274.42	/12.84	/29.32
7	98320.16	/0	/0	98298.66	98280.17
		98320.16	98320.16	/21.5	/39.99
8	112365.9	/0	/0	112319.27	112306.32
		112365.9	112365.9	/46.63	/59.58
9	126411.64	/0	/0	126313.25	126302.42
		126411.64	126411.64	/98.39	/109.22
10	140457.37	/15.58	/10.07	140303.54	140217.94
		140441.79	140447.3	/153.46	/239.43
11	154503.11	/85.61	/68.97	154111.64	154128.72
		154417.5	154434.14	/391.47	/374.39
12	168548.85	/99.29	/73.88	167967.46	167901.04
		168449.56	168474.97	/581.39	/647.81
13	182594.59	Infeasible	Infeasible	Infeasible	Infeasible

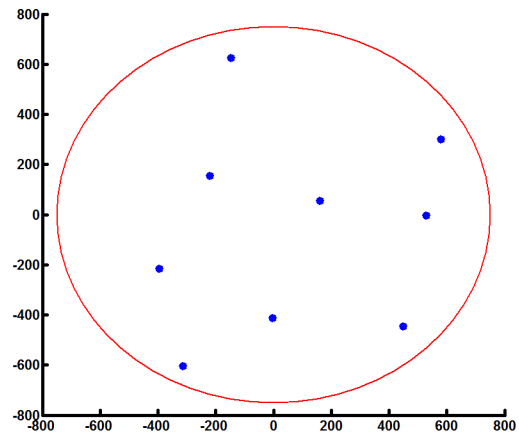
419

Table 6: Expected power and wake loss (*in kW*) in the wind farm of radius 750 (*m*) for the wind data set (II)

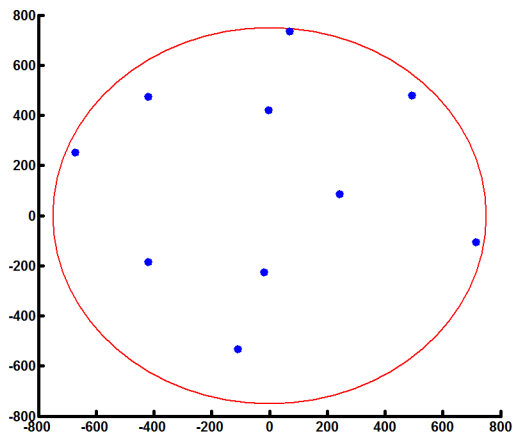
Number of turbines	Ideal	BBO (best)		BBO (average of 10-run)	
		/Wake Loss		/Wake Loss	
		50 N_p	100 N_p	50 N_p	100 N_p
2	14631.37	14631.37 /0	14631.37 /0	14631.37 /0	14631.37 /0
3	21947.06	21947.06 /0	21947.06 /0	21947.06 /0	21947.06 /0
4	29262.75	29262.75 /0	29262.75 /0	29262.75 /0	29262.75 /0
5	36578.44	36578.44 /0	36578.44 /0	36578.44 /0	36578.44 /0
6	43894.12	43894.12 /0	43894.12 /0	43877.4 /16.72	43852.33 /41.79
7	51209.81	51209.81 /0	51209.81 /0	51164.73 /45.08	51154.82 /54.99
8	58525.50	58525.50 /0	58525.50 /0	58435.71 /89.79	58428.48 /97.02
9	65841.19	65841.05 /0.14	65841.19 /0	65764.34 /76.85	65742.68 /98.51
10	73156.87	73156.67 / 0.20	73156.87 /0	73044 /112.87	72942.28 /214.59
11	80472.56	80456.48 /16.08	80457.35 /15.21	80216.84 /255.72	80090.17 /382.39
12	87788.25	87736.94 /51.31	87738.34 /49.91	87486.39 /301.86	87276.02 /512.23
13	95103.94	Infeasible	Infeasible	Infeasible	Infeasible



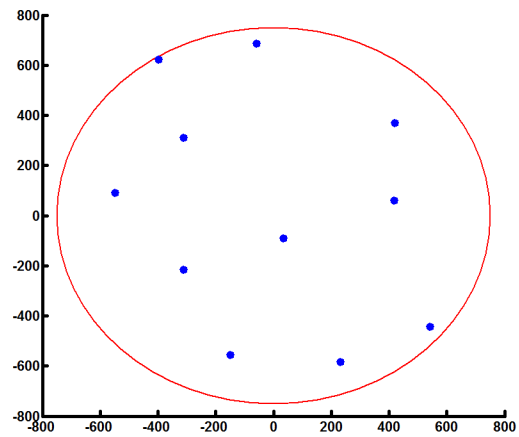
(a) 8 turbine



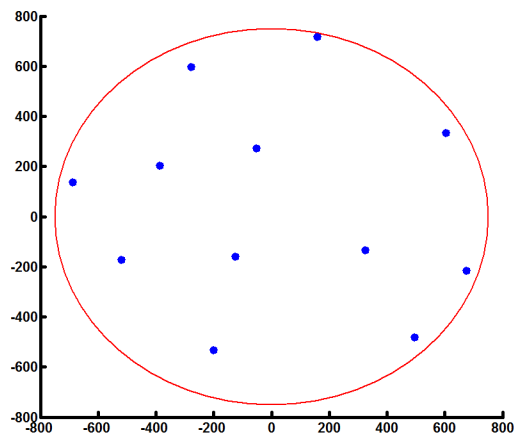
(b) 9 turbine



(c) 10 turbine

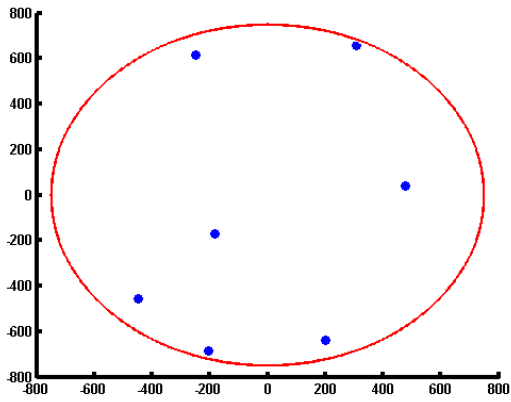


(d) 11 turbine

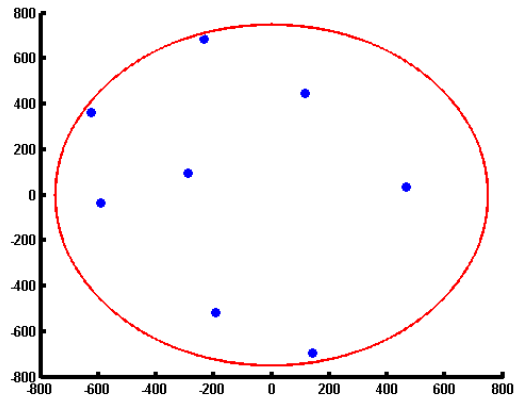


(e) 12 turbine

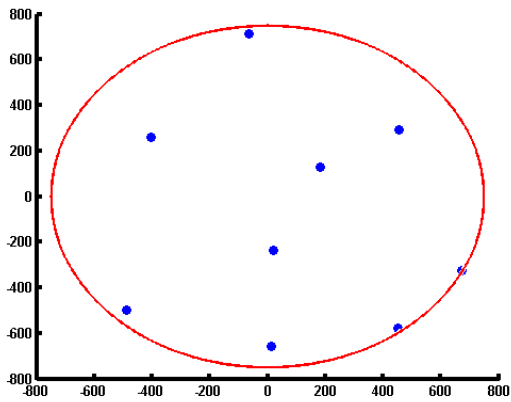
Figure 9: Turbines' location in the wind farm of radius 750 (m) for the wind data set (I)



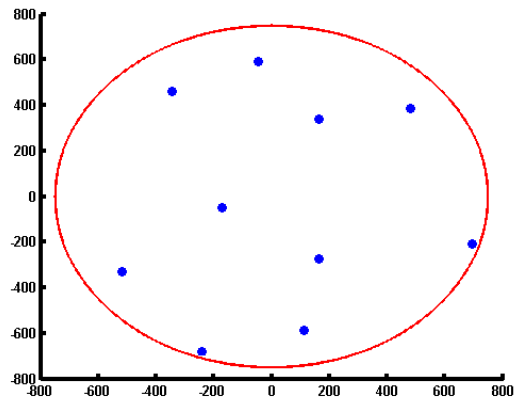
(a) 7 turbine



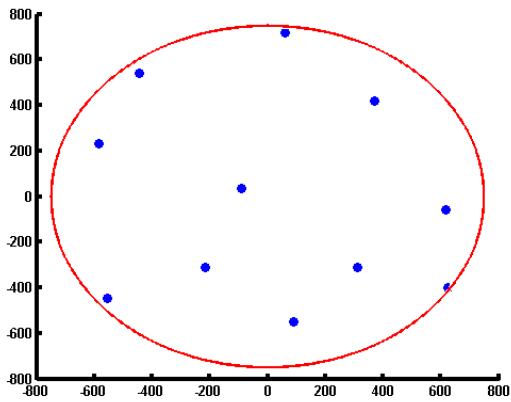
(b) 8 turbine



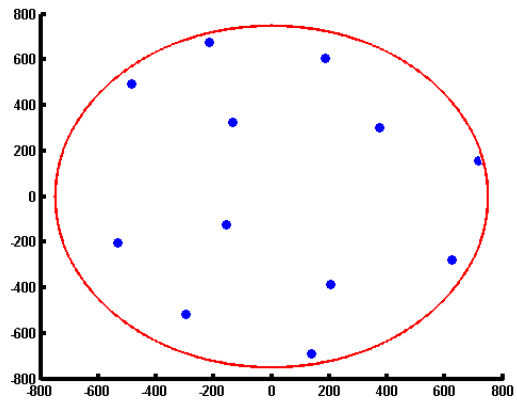
(c) 9 turbine



(d) 10 turbine

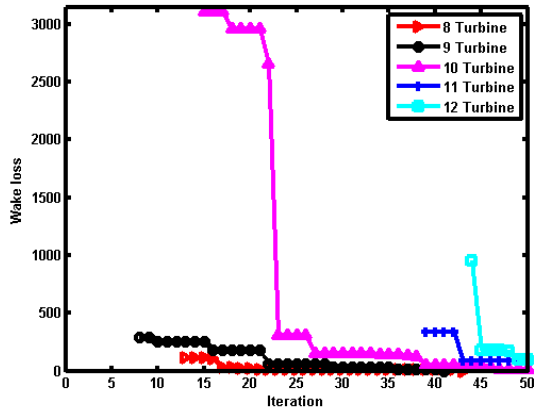


(e) 11 turbine

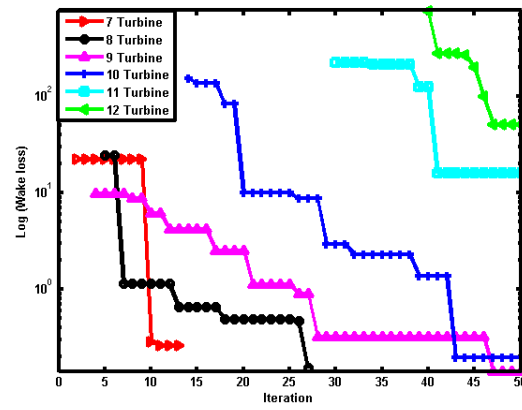


(f) 12 turbine

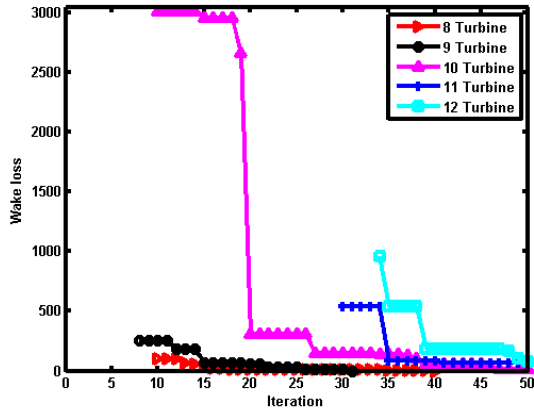
Figure 10: Turbines' location in the wind farm of radius 750 (m) for the wind data set (II)



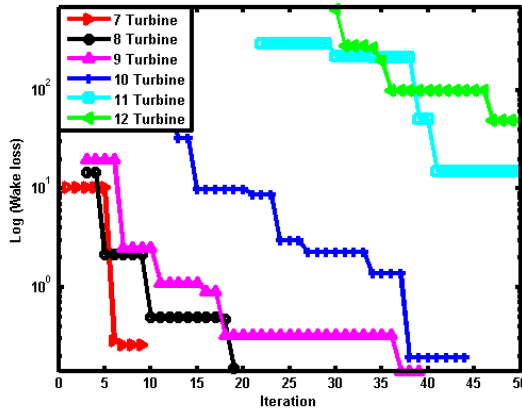
(a) Wake loss vs iteration for the wind data set (I)



(b) Wake loss vs iteration for the wind data set (II)

Figure 11: Fitness curve for the wind farm of radius 750 (m) with $N_p = 50$ 

(a) Wake loss vs iteration for the wind data set (I)



(b) Wake loss vs iteration for the wind data set (II)

Figure 12: Fitness curve for the wind farm of radius 750 (m) with $N_p = 100$

420

421 **Wind farm radius 1000 (m):** The same challenge is arises if we increase the farm
 422 radius. Again we need to search the maximum possible limit of the feasible number of
 423 turbines for the best-expected power in the wind farm of radius 1000 (m). In Tables
 424 7 and 8, columns 1 and 2 report the number of turbines and the ideal expected power
 425 corresponding to the number of turbines. In Tables 7 and 8, columns 3 and 4 report the
 426 best-expected power with wake loss for 50 population size ($50 N_p$) and 100 population
 427 size ($100 N_p$) corresponding to the number of turbines using BBO algorithm. Finally in
 428 Tables 7 and 8, columns 5 and 6 report the average of expected power with wake loss in
 429 10 runs for 50 population size ($50 N_p$) and 100 population size ($100 N_p$) corresponding
 430 to the number of turbines by BBO algorithm. Tables 7 and 8 illustrate the best-expected
 431 power, expected power of average of 10-run and wake losses up to 15 number of turbines

432 for the wind data set (I) and the wind data set (II), respectively. The developed data is
433 compared with the ideal expected power (optimum) given in Tables 7 and 8. Tables 7
434 and 8 illustrate the best-expected power and wake loss for exceeded number of turbines.
435 Here in this wind farm the best-expected power is same as the ideal expected power
436 until 11 number of turbines and the wind farm capacity is increased up to 15 number
437 of turbines given in Tables 7 and 8. Therefore, in this wind farm number of the feasible
438 turbines can not be exceeded by 15. So from the above study and experiments, BBO
439 algorithm is able to declare the maximum limit of the feasible wind turbines on the
440 selected wind farm.

441 Fig. 13, illustrates the optimum location of wind turbines from 10 to 15 turbines. Here
442 in figures 13(a)-13(f), turbines' best position is seen for the best-expected power (column
443 3) given in Table 7. Again Fig. 14, illustrates the optimum location of wind turbines
444 from 9 to 15 number of turbines. Here in figures 14(a)-14(g), turbines' best position is
445 seen for the best-expected power (column 3) given in Table 8.

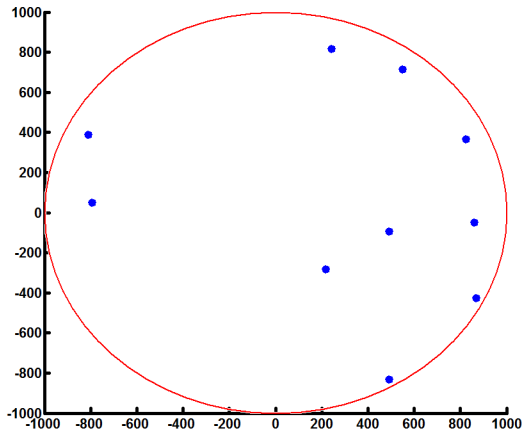
446 Similar to 500 (m) and 750 (m) farm cases, fitness curves are shown in figures 15 and
447 16.

Table 7: Expected power and wake loss (*in kW*) in the wind farm of radius 1000 (*m*) for the wind data set (I)

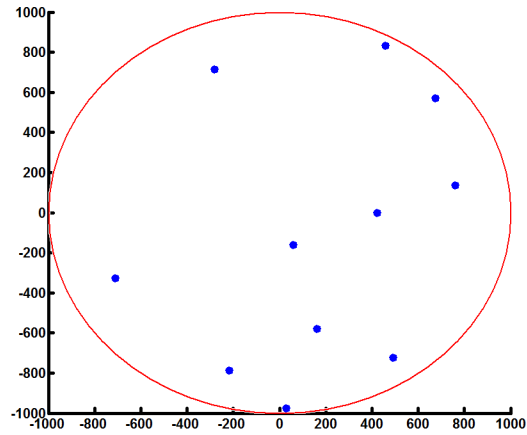
Number of turbines	Ideal	BBO (best)		BBO (average of 10-run)	
		/Wake Loss		/Wake Loss	
		50 N_p	100 N_p	50 N_p	100 N_p
2	28091.47	28091.47	28091.47	28091.47	28091.47
3	42137.21	/0	/0	/0	/0
		42137.21	42137.21	42137.21	42137.21
4	56182.95	/0	/0	/0	/0
		56182.95	56182.95	56182.95	56182.95
5	70228.69	/0	/0	/0	/0
		70228.69	70228.69	70228.69	70228.69
6	84274.42	/0	/0	/0	/0
		84274.42	84274.42	84274.42	84274.42
7	98320.16	/0	/0	/0	/0
		98320.16	98320.16	98320.16	98320.16
8	112365.9	, 112365.9	, 112365.9	112347.31	112338.35
		/0	/0	/18.59	/27.55
9	126411.64	126411.64	126411.64	126359.91	126333.03
		/0	/0	/51.73	/78.61
10	140457.37	140457.37	140457.37	140369.66	140354.84
		/0	/0	/87.71	/102.53
11	154503.11	154503.11	154503.11	154403.31	154379.54
		/0	/0	/99.8	/123.57
12	168548.85	168541.16	168547.77	168380.92	168355.41
		/7.69	/1.08	/167.93	/193.44
13	182594.59	182551.17	182552.78	182365.8	182304.01
		/43.42	/41.81	/228.79	/290.58
14	196640.32	196580.96	196583.66	196308.78	196264.54
		/59.36	/56.66	/331.54	/375.78
15	210686.06	210634.57	210634.57	210288.44	210237.57
		/51.49	/51.49	/397.62	/448.49
16	224731.8	Infeasible	Infeasible	Infeasible	Infeasible

Table 8: Expected power and wake loss (*in kW*) in the wind farm of radius 1000 (*m*) for the wind data set (II)

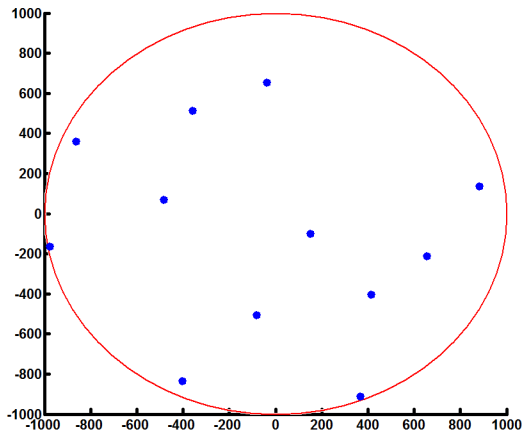
Number of turbines	Ideal	BBO (best)		BBO (average of 10-run)	
		/Wake Loss		/Wake Loss	
		50 N_p	100 N_p	50 N_p	100 N_p
2	14631.37	14631.37	14631.37	14631.37	14631.37
3	21947.06	21947.06	21947.06	21947.06	21947.06
4	29262.75	29262.75	29262.75	29262.75	29262.75
5	36578.44	36578.44	36578.44	36578.44	36578.44
6	43894.12	43894.12	43894.12	43894.12	43894.12
7	51209.81	51209.81	51209.81	51190.72	51182.14
8	58525.50	58525.50	58525.50	58487.53	58475.62
9	65841.19	65841.19	65841.19	65789.51	65762.46
10	73156.87	73156.87	73156.87	73065.24	73046.09
11	80472.56	80472.56	80472.56	80355.47	80337.34
12	87788.25	87768.71	87769.37	87595.63	87546.56
13	95103.94	94980.22	94980.75644	94854.4	94785.18
14	102419.62	102249.93	102252.0039	102058.08	102023.84
15	109735.31	109504.22	109505.8813	109327.72	109266.6
16	117051	Infeasible	Infeasible	Infeasible	Infeasible



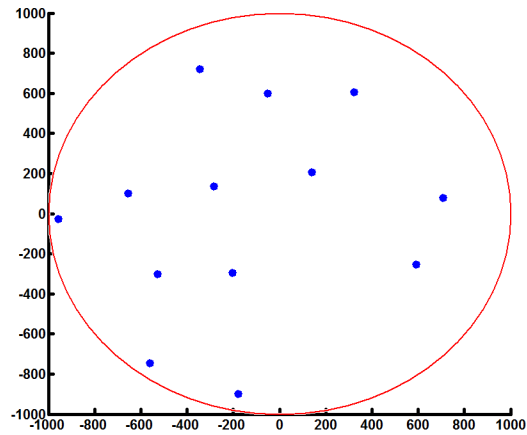
(a) 10 turbine



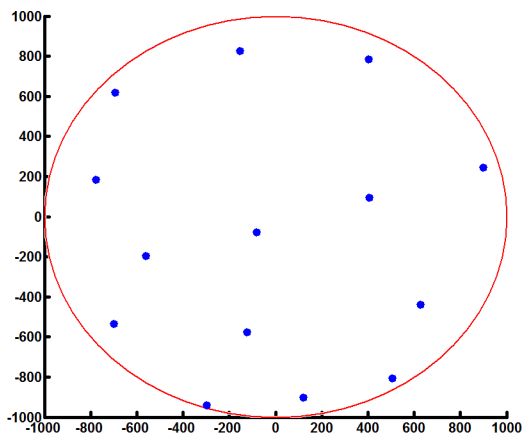
(b) 11 turbine



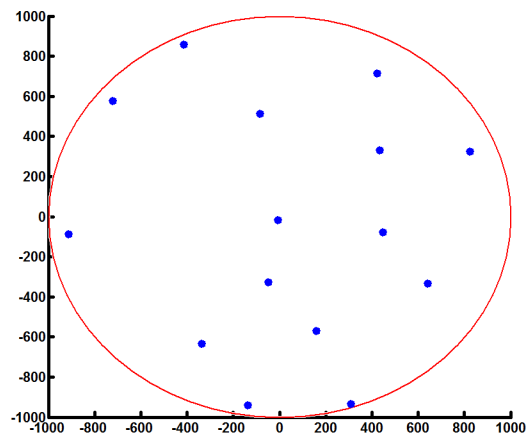
(c) 12 turbine



(d) 13 turbine

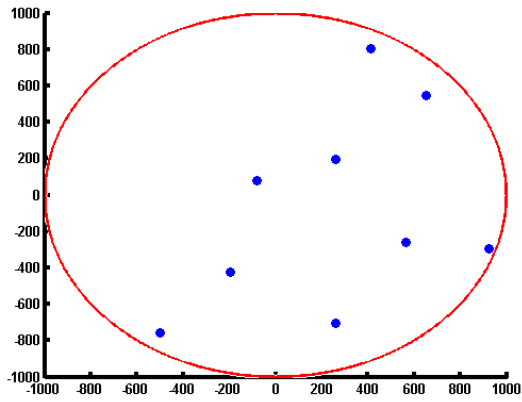


(e) 14 turbine

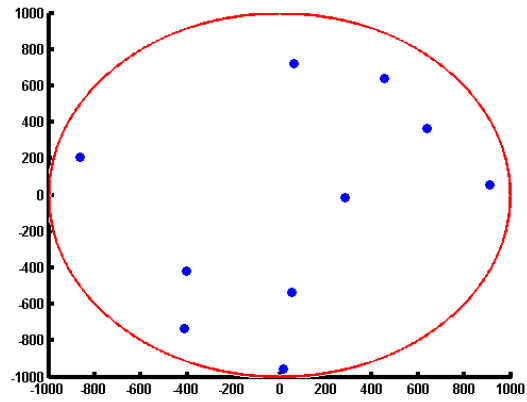


(f) 15 turbine

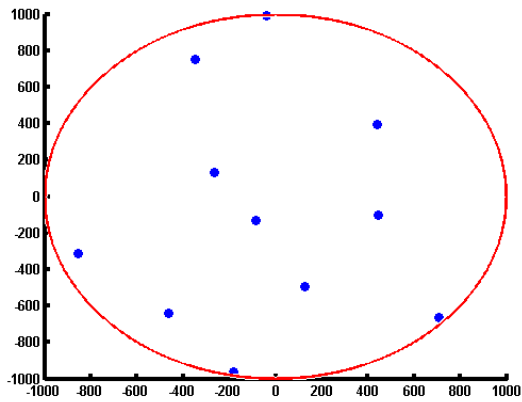
Figure 13: Turbines' location in the wind farm of radius 1000 (m) for the wind data set (I)



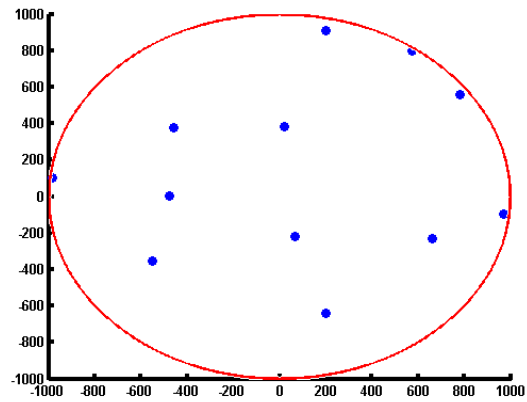
(a) 9 turbine



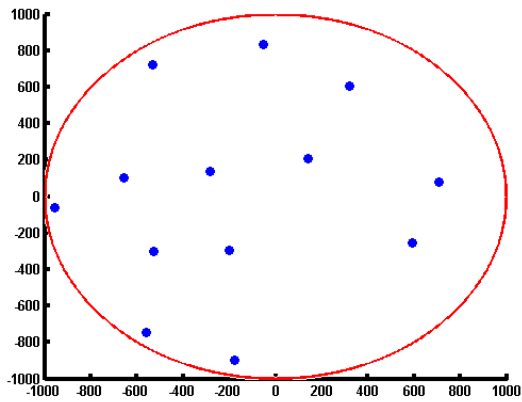
(b) 10 turbine



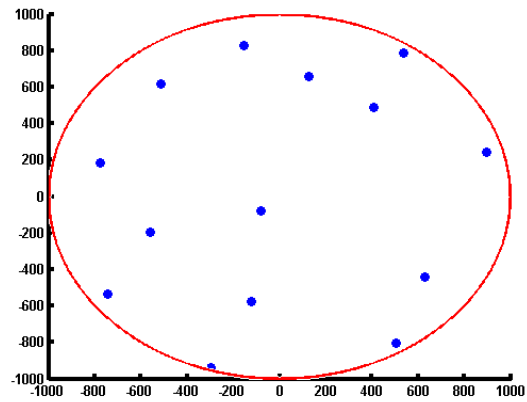
(c) 11 turbine



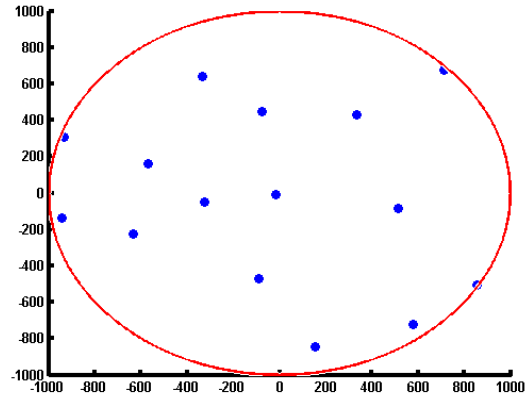
(d) 12 turbine



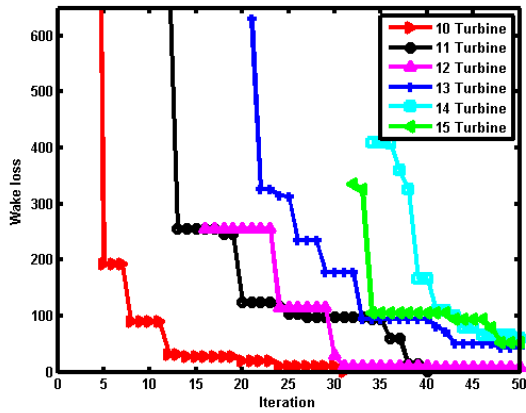
(e) 13 turbine



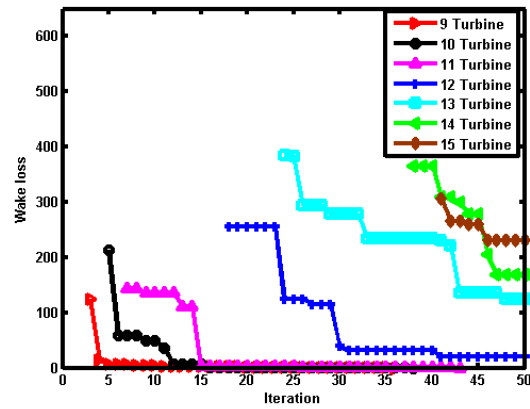
(f) 14 turbine



(g) 15 turbine

Figure 14: Turbines' location in the wind farm of radius 1000 (m) for the wind data set (II)

(a) Wake loss vs iteration for the wind data set (I)



(b) Wake loss vs iteration for the wind data set (II)

Figure 15: Fitness curve for the wind farm of radius 1000 (m) with $N_p = 50$

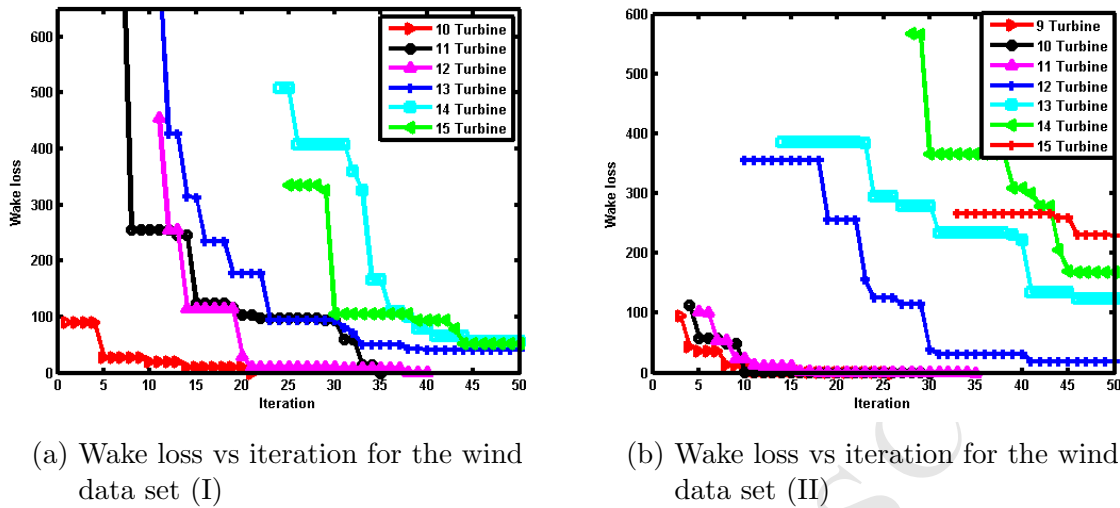


Figure 16: Fitness curve for the wind farm of radius 1000 (m) with $N_p = 100$

448 6. Conclusion

449 In this paper, WFLOP (wind farm layout optimization problem) is considered to
 450 solve using BBO. The main objective of WFLOP is to maximize the energy production
 451 along with the reduction of wake effect challenge. In this article, three different circular
 452 wind farms with radii 500 (m), 750 (m) and 1000 (m) are considered. The performance
 453 of BBO algorithm was evaluated on two wind data sets (wind data set (I) with constant c
 454 and wind data set (II) with non-constant c). This paper also recommends the maximum
 455 possible number of wind turbines which can be placed in a wind farm without any
 456 wake loss. Numerical experiments conclude that BBO is able to find the better optimal
 457 placement of wind turbines in the wind farms without any wake loss than prior studies.
 458 Earlier methodologies can fit maximum 3 turbines in a farm of radius 500 (m) while
 459 BBO can fit maximum 7 turbines in the same farm without any wake loss. Similarly,
 460 BBO outperforms for other sizes of wind farms.
 461 Thus BBO is recommended as an efficient solver for WFLOP.

462 7. Acknowledgment

463 The second author acknowledges the funding from South Asian University, New
 464 Delhi, India to carry out this research.

465 References

- 466 [1] M. A. Lackner, C. N. Elkinton, An analytical framework for offshore wind farm
 467 layout optimization, *Wind Engineering* 31 (1) (2007) 17–31.
- 468 [2] J. C. Mora, J. M. C. Barón, J. M. R. Santos, M. B. Payán, An evolutive algorithm
 469 for wind farm optimal design, *Neurocomputing* 70 (16) (2007) 2651–2658.
- 470 [3] C. N. Elkinton, J. F. Manwell, J. G. McGowan, Algorithms for offshore wind farm
 471 layout optimization, *Wind Engineering* 32 (1) (2008) 67–84.

- 472 [4] G. Mosetti, C. Poloni, B. Diviacco, Optimization of wind turbine positioning in
473 large windfarms by means of a genetic algorithm, *Journal of Wind Engineering and*
474 *Industrial Aerodynamics* 51 (1) (1994) 105–116.
- 475 [5] S. Grady, M. Hussaini, M. M. Abdullah, Placement of wind turbines using genetic
476 algorithms, *Renewable energy* 30 (2) (2005) 259–270.
- 477 [6] H.-S. Huang, Distributed genetic algorithm for optimization of wind farm annual
478 profits, in: *Intelligent Systems Applications to Power Systems, 2007. ISAP 2007.*
479 *International Conference on, IEEE, 2007*, pp. 1–6.
- 480 [7] A. Emami, P. Noghreh, New approach on optimization in placement of wind tur-
481 bines within wind farm by genetic algorithms, *Renewable Energy* 35 (7) (2010)
482 1559–1564.
- 483 [8] S. Şişbot, Ö. Turgut, M. Tunç, Ü. Çamdalı, Optimal positioning of wind turbines
484 on gökçeada using multi-objective genetic algorithm, *Wind Energy* 13 (4) (2010)
485 297–306.
- 486 [9] M. Samorani, The wind farm layout optimization problem, in: *Handbook of Wind*
487 *Power Systems*, Springer, 2013, pp. 21–38.
- 488 [10] U. A. Ozturk, B. A. Norman, Heuristic methods for wind energy conversion system
489 positioning, *Electric Power Systems Research* 70 (3) (2004) 179–185.
- 490 [11] M. Bilbao, E. Alba, Simulated annealing for optimization of wind farm annual
491 profit, in: *Logistics and Industrial Informatics, 2009. LINDI 2009. 2nd International,*
492 *IEEE, 2009*, pp. 1–5.
- 493 [12] R. A. Rivas, J. Clausen, K. S. Hansen, L. E. Jensen, Solving the turbine positioning
494 problem for large offshore wind farms by simulated annealing, *Wind Engineering*
495 33 (3) (2009) 287–297.
- 496 [13] A. Kusiak, Z. Song, Design of wind farm layout for maximum wind energy capture,
497 *Renewable Energy* 35 (3) (2010) 685–694.
- 498 [14] M. Wagner, K. Veeramachaneni, F. Neumann, U.-M. O'Reilly, Optimizing the layout
499 of 1000 wind turbines, *European wind energy association annual event* (2011) 205–
500 209.
- 501 [15] P.-Y. Yin, T.-Y. Wang, A grasp-vns algorithm for optimal wind-turbine placement
502 in wind farms, *Renewable Energy* 48 (2012) 489–498.
- 503 [16] Y. Eroğlu, S. U. Seckiner, Design of wind farm layout using ant colony algorithm,
504 *Renewable Energy* 44 (2012) 53–62.
- 505 [17] Y. Eroğlu, S. U. Seckiner, Wind farm layout optimization using particle filtering
506 approach, *Renewable Energy* 58 (2013) 95–107.
- 507 [18] J. F. Manwell, J. G. McGowan, A. L. Rogers, *Front Matter*, Wiley Online Library,
508 2002.

- 509 [19] N. O. Jensen, A note on wind generator interaction, 1983.
- 510 [20] I. Katic, J. Højstrup, N. Jensen, A simple model for cluster efficiency, in: European
511 Wind Energy Association Conference and Exhibition, 1986, pp. 407–410.
- 512 [21] H. Neustadter, D. Spera, Method for evaluating wind turbine wake effects on wind
513 farm performance, *Journal of Solar Energy Engineering* 107 (3) (1985) 240–243.
- 514 [22] D. W. Stroock, A concise introduction to the theory of integration, Springer Science
515 & Business Media, 1999.
- 516 [23] D. Simon, Biogeography-based optimization, *Evolutionary Computation, IEEE*
517 *Transactions on* 12 (6) (2008) 702–713.
- 518 [24] R. H. MacArthur, E. O. Wilson, *The theory of island biogeography*, Vol. 1, Prince-
519 ton University Press, 1967.

Highlights:

- Wind Farm Layout Optimization Problem (WFLOP) is solved using Biogeography-Based Optimization (BBO) method.
- The problem has been dealt in two ways:
 - For a given wind farm and given number of wind turbines, finding the optimal location of wind turbines.
 - Finding the maximum number of wind turbines and their locations, which can be accommodated for a given size of wind farm.
- The experiments have been performed with 500m, 750m and 1000m farm radii and with two different wind data sets having constant and non-constant weibull distribution scale parameter c .
- Results have been compared and analyzed with earlier published results.
- The proposed approach has been proved to be competitive for solving WFLOP.